3D Face Recognition Using Two Views Face Modeling and Labeling

Yi Sun and Lijun Yin
Computer Science Department
State University of New York at Binghamton
Binghamton, New York 13902 USA

Abstract

The ability to distinguish different people by using 3D facial information is an active research problem being undertaken by the face recognition community. In this paper, we propose to use a generic model to label the 3D facial features. This approach relies on our realistic face modeling technique, by which the individual face model is created using a generic model and two views of a face. In the individualized model, we label the face features by their maximum and minimum curvatures. Among the labeled features, the "good features" are selected by using a Genetic Algorithm based approach. The feature space is then formed by using these new 3D shape descriptors, and each individual face is classified according to its feature space correlation. We applied 72 individual models for the test. The experimental results show that the shape information obtained from the 3D individualized model can be used to classify and identify individual facial surfaces. The rank-four correct recognition rate is about 92%. The 3D individualized model provides consistent and sufficient details to represent individual faces while using a much more simplified representation than the range data models. This work provides the possibility to reduce the complexity of 3D data processing, and is feasible for real applications such as in a non-cooperative imaging circumstance or in the situation when range data using 3D scanners are not possible to acquire.

1. Introduction

3D face recognition has attracted much attention in recent years [4, 6-12, 18, 21]. It seems to be superior to 2D face recognition due to its less affection by imaging conditions and facial pose variations [1, 3]. Currently, most research for exploring 3D face information focuses on the investigation of 3D range data obtained by 3D digitizers due to the difficulty of 3D reconstruction from 2D images [7, 21, 2, 9]. Despite its high fidelity representation of faces, 3D range data is not feasible for many application scenarios. Firstly, an ideal environment with the cooperation of subjects is needed to capture 3D information using a 3D scanner. Secondly, the range data obtained is usually in a raw format, and different persons' faces may have a different number of vertices. It is hard to compare from face to face without building consistent correspondences between two subjects. Therefore, further processing is needed in order to extract the feature regions and segment the facial surface. Finally, although the high-resolution range data provides a realistic appearance that is good for perception and animation in the entertainment industry, it contains redundant information, which may be unnecessary or could make the face shape comparison noise sensitive.

In order to reduce the complexity of data processing and to provide the model correspondence easily, a template model could be used for fitting a generic model to the face image [15, 16]. Currently, there are some successful systems that utilize 3D wire-frame models to represent the face shape for recognition. However, the accuracy of 3D feature representation is still limited by the selected simple models in which only a small number of vertices are presented. Thus it is hard to label the face surface and characterize its property precisely.

In this paper, we present a more accurate face representation method using a generic model with about 3000 vertices. The utilization of the face model with certain accuracy can help us to describe the face surface more precisely. We label the face surface by its principal curvatures based on the generated individual facial model. Since every individualized model has the same number of vertices, the correspondence between different individual models is inherently kept. And thus, the 3D shape comparison can be carried out easily.

Figure 1 shows the general framework of our proposed system. In this system, a 3D face model database is firstly created based on two views of face images of each subject and a generic face model. Then we implement a cubic approximation method on each 3D individualized model to analyze the principal curvatures (i.e., the maximum and minimum curvatures at each vertex's location). After labeling the facial surface by using 8 categories of surface types (e.g., concave, convex, saddle, etc.), we are able to segment different regions and extract the 3D shape descriptors using their surface features. These 3D shape descriptors are the simplified representation of each facial instance, which preserve the surface varieties of different faces. Among the

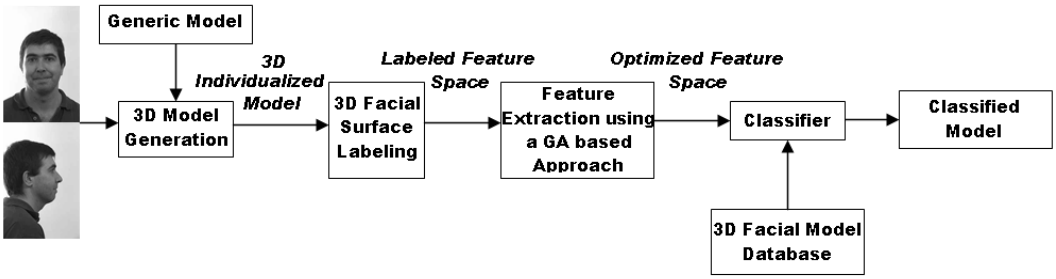

Figure 1: Framework of proposed 3D face labeling and recognition system (images in the left are provided by FERET[14])

3D descriptors, only the partial features ("good features") are selected. We apply a feature selection procedure based on the Genetic Algorithm to form a feature vector that is composed of the selected "good features". As a result, the dimension of the 3D descriptors is greatly reduced. Finally, the composed new feature vectors are used for a similarity measurement to classify individual facial models based on their feature space correlations.

The paper is organized as follows: the 3D face model database creation using our existing face modeling tool is introduced in Section 2. The algorithms for face model labeling and the good feature selection are described in Section 3 and Section 4, respectively. Section 5 explains the similarity measurement using the feature space correlation, followed by the experiments and performance analysis in Section 6. Finally, the concluding remarks are given in Section 7.

2. 3D facial model database creation

Based on our existing work [13], we created a 3D facial model database by modifying a generic facial model to customize the individual person's face, given two views of images, i.e., a front view and a side view of the face. This approach is based on recovering the structure of selected feature points in the face and then adjusting a generic model using these control points to obtain the individualized 3D head model. The algorithm is implemented by three major components. First of all, a set of fiducial points are extracted from a frontal view and a side view of face images using a maximum curvature tracing algorithm. Then, the generic face model is adjusted to fit the face images in two views separately. The model fitting process is based on the dynamic interpolation approach using the extracted fiducial points. Finally, the two view's models are combined together to generate the individualized 3D facial model. The blended textures from the two views are synthesized and mapped onto the instantiated model to generate the face images in arbitrary views. Our generic wire-frame facial model consists of 2953 vertices, which represent the face surface with sufficient accuracy. This model instantiation approach is simple and efficient. The created model is accurate enough to characterize features of the individual face. Our 3D face model database is generated using 105 pairs of face images from 40 subjects. These source image pairs are mainly chosen from the database of FERET [14] and XM2VTS [22], and some additional images are captured by our research group. For each subject, there are two or three pairs of frontal and profile images, which were taken under different imaging conditions (e.g., different poses, lighting, hair style and facial appearances at different time periods). We created two or three instance models for each subject, and in total there consists of 105 individual instance models in our database. Figure 2 shows three examples of the generated models in the database.

3. 3D facial model labeling

In order to better characterize 3D features of the facial surface, each vertex on the individual model is labeled by one of the label types (i.e., convex peak, convex cylinder/cone, convex saddle, minimal surface, concave saddle, concave cylinder/cone, concave pit and planar). Therefore, the facial model is represented by a set of labels. Our labeling approach is based on the estimation of principal curvatures of the facial surface. Curvature has desirable computational and perceptual characteristics [2, 5], which is independent of rigid transformation. It is believed that the curvature information is a good reflection of local shapes of the facial surface.

Given a face mesh model of vertices and polygons approximating the facial smooth surface, we need to calculate accurate estimates of the principal curvatures and their directions at points on the facial surface. There are a number of methods for estimating the principal curvatures and principal directions of the underlying surface, including the normal curvature approximation, quadratic surface approximation, cubic approximation and the higher order methods [17]. Since the estimation is performed on the sparse mesh model rather than the dense range data model, the mi-

image instance I | model instance-I | image instance II | model instance-II

Figure 2: Example of 3D model database created from the frontal and profile views of each subject. Row 1 to Row 3 show three subjects, each subject has two instance models.

nor normal curvature approximation errors could be magnified into large errors in the estimated principal directions. Therefore we need to choose a high order approximation method. Considering the trade-off between the estimation accuracy and the computation complexity, we adopt the cubic approximation approach to calculate the principal curvatures and their directions on each vertex of the 3D model. The calculation is briefly described as follows: Let p denote a point on a surface $\boldsymbol{S}$, $N_p$denote the unit normal to $\boldsymbol{S}$ at point p, and $X(u, v)$ be a local parameterization of $\boldsymbol{S}$ at p. Using $X_u(p)$, $X_v(p)$ and N_p as a local coordinate system, we can obtain the principal curvatures and the principal directions by computing the eigenvalues and eigenvectors of the Weingarten curvature matrix:

$$W = \begin{pmatrix} \frac{eG-fF}{EG-F^2} & \frac{fE-eF}{EG-F^2} \\ \frac{fG-gF}{EG-F^2} & \frac{gE-fF}{EG-F^2} \end{pmatrix} \quad (1)$$

Where

$$\begin{array}{ll} e = N_p \cdot X_{uu}(p) & E = X_u(p) \cdot X_u(p) \\ f = N_P \cdot X_{uv}(p) & F = X_u(p) \cdot X_v(p) \\ g = N_p \cdot X_{vv}(p) & G = X_v(p) \cdot X_v(p) \end{array}$$

The eigenvalues $\lambda_1$and λ_2 of the matrix W are the maximum and minimum principal curvatures of the surface $\boldsymbol{S}$ at point p. The eigenvectors $\boldsymbol{v}_1$ and $\boldsymbol{v}_2$, which are represented in a global coordinate system, are the corresponding maximum and minimum principal directions. In order to estimate the Weingarten curvature matrix accurately, we apply the cubic approximation approach to fit a local cubic surface onto the face model surface centered on each vertex. To do so, we firstly transform the adjacent vertices of p to a local system with the origin at p and with the positive z axis along the estimated normal N_p. Based on the cubic surface equation, we can derive its surface normal and establish two equations for each normal. Then a linear regression method can be applied to solve the equation groups [17], and the elements of the Weingarten matrix can be determined (see detail in [17]). Figure 3 shows one example of the obtained maximum and minimum principal directions for the vertices of the generic face model.

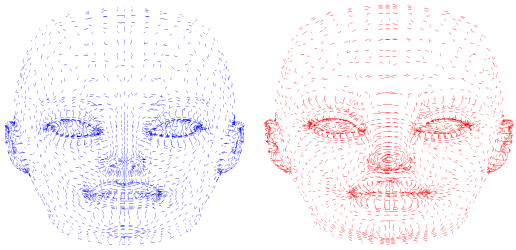

Figure 3: Principal directions for the vertices of a generic 3D model. Left: the minimum principal directions; Right: the maximum principal directions.

After estimating the principal curvatures and the directions of each vertex, we can further categorize each vertex into one of the eight distinct label types. The labels are classified according to the relation of the principal curvatures, which are expounded in Table 1.

Since every vertex is represented by a surface label, each labeled vertex provides a feature component in the facial feature space. The reason that we use the surface labeling to represent the local shape on each vertex is that the surface type determined by the curvatures is stable to the location of each vertex and is relatively insensitive to the small shape distortion when compared to the other feature representations, such as the vertex's coordinates, curvature value itself and other geometric measurements (e.g., distance, an-

(1)	Convex peak	$\lambda_1 < 0\ \lambda_2 < 0$
(2)	Convex Cylinder	$\lambda_1 = 0\ \lambda_2 < 0$
(3)	Convex Saddle	$\lambda_1 > 0\ \lambda_2 < 0\ \|\lambda_1\| < \|\lambda_2\|$
(4)	Minimal Surface	$\|\lambda_1\| = \|\lambda_2\|$
(5)	Concave Saddle	$\lambda_1 > 0\ \lambda_2 < 0\ \|\lambda_1\| > \|\lambda_2\|$
(6)	Concave Cylinder	$\lambda_2 = 0\ \lambda_1 < 0$
(7)	Concave Pit	$\lambda_1 > 0\ \lambda_2 > 0$
(8)	Planar	$\lambda_1 = 0\ \lambda_2 = 0$

Table 1: Eight kinds of facial surface labels classified by their principal curvatures.

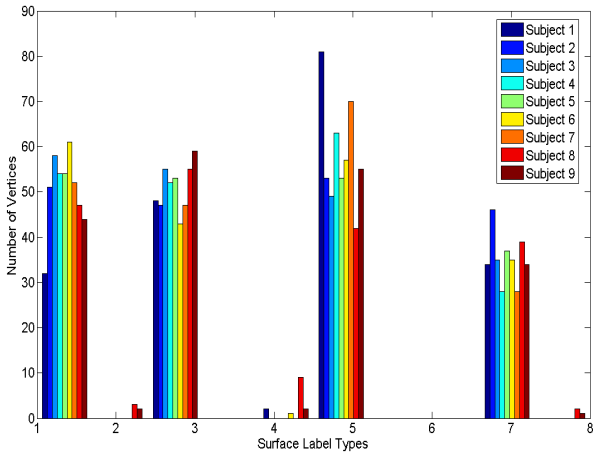

(a)

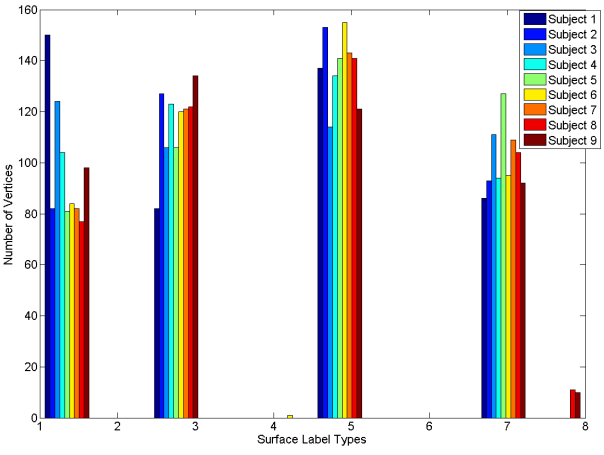

(b)

Figure 4: Histograms of the vertex label types in regions of (a) eyeballs and (b) eye-lids of nine subjects. (Eight label types 1-8 are defined in the Table 1).

gle, etc.) So, once the reconstruction from two orthogonal views of images to the 3D individualized model is accurate enough to preserve the curvature types of the vertices, it will not influence the classification result. The usage of surface labeling can help improve the robustness to the facial expression variation. We will illustrate this property in the section 6.

Figure 5(a) shows the result of surface labeling on the generic model using the cubic approximation method. Four label types (i.e., convex (peak), convex saddle, concave (pit) and concave saddle) are dominant on this model as a whole. In order to understand the label distribution on different regions of a face, we conduct histogram statistics on the different regions of the individual models. The statistical results show that different facial regions of the same subject have different distributions of the label types. Furthermore, the label distributions of the same facial region for different subjects are also clearly distinguishable. As an example, Figure 4 illustrates the label histograms of nine subjects' facial models on two selected regions (i.e., eyeballs and eyelids). As seen from (a) and (b), the label histograms in the same region are different from one person to another among the nine subjects, e.g., the dominant label in the region of eye-lids is the convex saddle for Subject 9, while it is the concave saddle for Subject 6. The label histograms are also different from region to region in the same subject's model, as compared between region (a) eyeballs and (b) eye-lids.

4. Good feature selection using a GA-based approach

After the stage of facial model labeling, each individual face model is represented by a set of labels (i.e., 2953 labeled vertices in each model). Among the set of labels, only the labels located in certain regions are of our most interest. Some non-feature labels could be noises that could blur the individual facial characteristics. Therefore, we need to apply a feature screening process to select features in order to better represent the individual facial traits for maximizing the difference between different subjects while minimizing the size of the feature space. We refer to the selected features as the "good features". In order to select the good features, we partition the face model into 15 sub-regions based on their physical structures(there are overlaps between some of the regions), which is similar to the region components used in [6], as expounded in Table 2 and Figure 5(b). These sub-regions represent the anatomic structure of the human face. However, they are not equally robust for characterizing the traits of each individual subject. For example, some regions are sensitive to local expression variation, and they may not be the good features for discriminating different faces.

Since not all the sub-regions contribute to the recogni-

R0	Eye brows	**R5**	Upper eye lid of the left eye	**R10**	Lower eye lids (R6+R8)
R1	Eye balls	**R6**	Lower eye lid of the left eye	**R11**	Eye lids (R9 + R10)
R2	Lip	**R7**	Upper eye lid of the right eye	**R12**	Frontal head contour
R3	Nose	**R8**	Lower eye lid of the right eye	**R13**	Central facial profile
R4	Mouth	**R9**	Upper eye lids (R5+R7)	**R14**	Chin contour

Table 2: Selected 15 sub-regions (R0 - R14) for feature extraction.

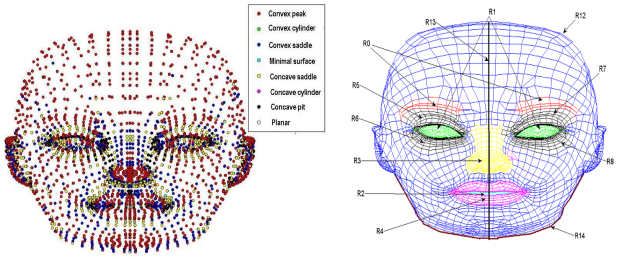

(a) (b)

Figure 5: (a) 3D model labeling using eight label types based on the principal curvatures. Each dot corresponds to one vertex, which is labeled by one color. (b) Sub-regions defined on the generic facial model.

tion task, and not all the vertices within one sub-region contribute to the classification, we need to select (1) the best set of vertex labels within each sub-region, and (2) the best set of sub-regions. The purpose of the feature selection is to remove the irrelevant or redundant features which may degrade the performance of face classification. Since it is a difficult task to examine all possible combinations of feature sets, an efficient strategy for optimal feature selection is highly necessary. The genetic algorithms (GA) have been used successfully to address this type of problem [24]. So we choose to use a GA-based method to select the components that contribute the most to our face recognition task. GA provides a learning method analogous to biological evolution. It is an evolutionary optimization approach which is an alternative to traditional optimization methods. GA is most appropriate for complex non-linear models in order to find the location of the global optimum [19]. The solution of GA is identified by a fitness function where the local optima are not distinguished from other equally fit individuals. Those solutions closer to the global optimum will have higher fitness values, and the outcomes will tend to get closer to the global optimum. Here, we chose to use the Equal Error Rate (EER) as the fitness function. For each sub-region, we obtained an EER when we performed the face similarity measurement based on the sub-region only, given the training set of the 3D face model database. The similarity measurement is based on the feature space's correlation, which will be introduced in the next section. The procedure for the feature selection consists of two parts: (1) initialization for vertices selection in each sub-region and (2) the integration sub-regions.

1. *Vertices selection for each sub-region*

   The GA-based initialization is described by the following pseudo-procedure:

   Let the EER denote as a fitness function,
   Compute the fitness function for each chromosome and rank them.
   Feature space = the chromosome with the highest rank fitness value.
   For each chromosome left in the current sub-region:
   Do add it in the feature space, and
   Compute the EER of the feature space
   If EER has decreased
   Remove the added chromosome
   Keep the final regional feature space as the optimal feature space of the current sub-region.

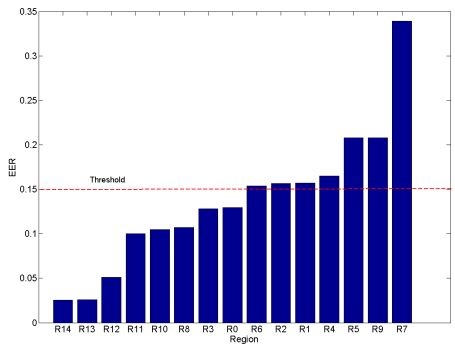

(a)

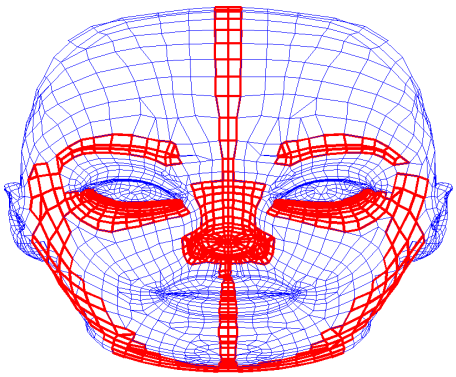

(b)

Figure 6: (a) EERs for 15 sub-regions which are sorted in a non-decreasing order; (b) The optimized feature space (marked with red color) after performing the GA-based method on the training set.

2. *The integration of sub-regions*

Following the previous step, all the sub-regions have been reduced to the regional feature spaces. At this point, we may use the EER to determine which regional feature spaces should be selected as our final feature spaces. Here we choose those regional feature spaces that have a high-ranking fitness value (EER) as the final feature space. Figure 6(a) shows the EER for each sub-region after the vertices are selected from the training set. Figure 6(b) depicts the selected sub-regions on the face model. Note that in this training stage, the EER values are obtained by testing on the training set, which contains 33 face models from 15 subjects.

We set the threshold at the EER value of 0.15 (i.e., the first 8 ranks) based on the mean of the fitness values. As a result, the first 8 sub-regions are selected, which are sub-regions 0, 3, 8, 10, 11, 12, 13 and 14 as shown in Figure 6(a) and (b). The numbers of vertices selected from the sub-regions are: 15 vertices for R0; 45 for R3; 11 for R8; 13 for R10; 23 for R11; 42 for R12; 15 for R13 and 21 for R14. Since there are overlaps for different regions, the optimized feature space contains 137 vertices. Although using a sub-region, R14 for instance, may achieve a lower EER rate, we think it contains too small number of vertices that are relatively sensitive to the selection of training data set and sensitive to the noise. Note that the optimized feature space represents the individual facial traits. Because the majority of these features are located in the "static" facial regions, the feature space is less influenced by the facial skin deformation caused by facial expressions.

5. Face model matching based on feature space correlation

After selecting the optimal features in the previous training stage, the components (i.e., vertex labels) in the final feature space form a feature vector for each individual facial model. The similarity of two individual facial models can be measured by the similarity of their feature vectors. The Euclidean distance and cross-product of two vectors could be the direct solutions to calculate the similarity score. However, by considering the statistical property of feature label space, we chose to use the correlation [23] to measure the similarity of two feature vectors. The usage of correlation-based similarity measurement is based on the observation that the facial surface primitive labels are highly correlated across the instances of the same individual. The computation of feature correlations can be described as follows: given two feature vectors X and Y from two individual models, $X = \{x_1, x_2, ..., x_m\}$ and $Y = \{y_1, y_2, ..., y_m\}$, where m is the number of vertices in the feature space. Each component of X and Y corresponds to each vertex individually, and each component is represented by one of the eight label types (denoted from 1 to 8). The correlation coefficient $\rho$is calculated by

$$\rho(X,Y) = \frac{\sum_{i=1}^{m}(x_i - \overline{x})(y_i - \overline{y})}{\sqrt{(\sum_{i=1}^{m}(x_i - \overline{x})^2) \cdot (\sum_{i=1}^{m}(y_i - \overline{y})^2)}} \quad (2)$$

The high correlation coefficient of two feature vectors indicates the high similarity of two individual models. As a result, the individual models can be simply classified according to their correlation values.

6. Experiments and analysis

In our 3D face model database, there are 40 subjects with total 105 instance models (note that each subject has two or three generated instance models depending on two or three pairs of instance images available.) We chose 33 generated instance models from 15 subjects as a training set, and 72 generated models from 25 subjects as a test set. As described in Section 4, after the training stage, 137 feature vertices are finally included in the optimal feature space.

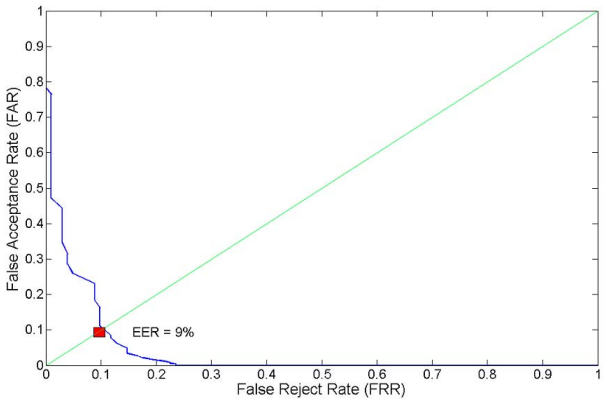

(a)

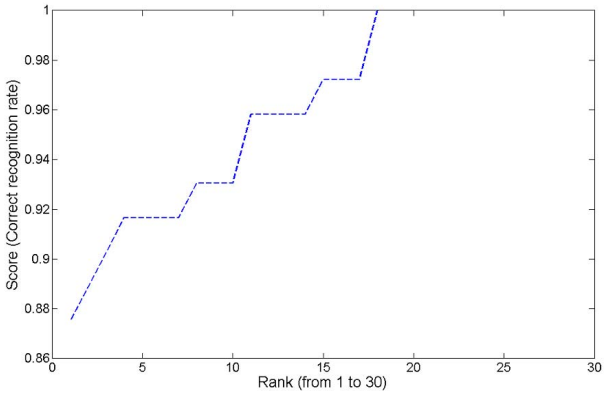

(b)

Figure 7: (a) ROC curve (marked with FAR, FRR, and EER) and (b) Accumulative score vs. rank

The performance of the 3D facial model classification is illustrated by a ROC curve, which is obtained by conducting the classification on the test set (72 instance models). As shown in Figure 7(a), the EER is 9%. Figure 7(b) shows the correct recognition rates using the score vs. rank curve. Our system can achieve a 92% correct recognition rate if the first four candidates (rank=4) are selected. In order to investigate how critical the facial expression could affect the feature space and how well our feature labels could represent the individual characteristics, we compared both the labeled models from different subjects and the models from different expressions of the same subject. Among our test set, the feature space difference between expression models of the same subject is much smaller than the difference between the different subjects. Figure 8 shows one example with two different subjects (i.e., one subject has one instance model (a) and the other has two instance models (b-c) with two different expressions). As seen in the nose region (marked with a black box), the distribution of feature labels has a distinct pattern in (a) as compared to the patterns in (b) and (c). The label compositions of (b) and (c) are very similar although the nose shape has been changed because of the smiling expression. This suggests that without large expressional variations, the similarity between models of the same subject (intra-class) is higher than the similarity between models of different subjects (intra-class). The reason for that lies in (1) the surface labeling at each vertex location is stable to the surface change if the expression is performed in a non-exaggerate fashion and (2) the set of good features selected by our system are less affected by the expression change.

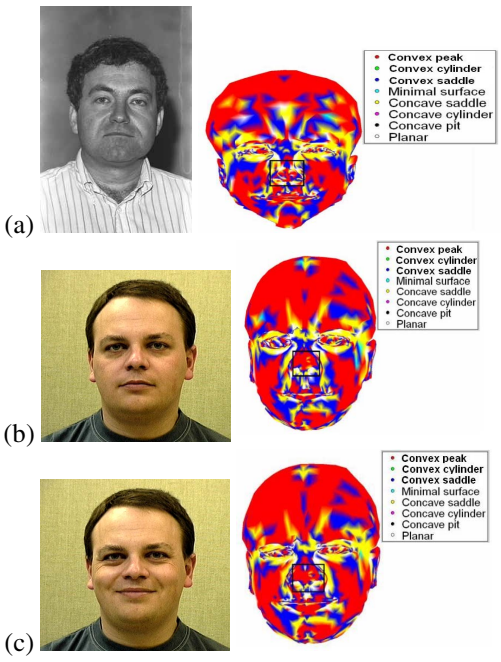

Figure 8: Example of two subjects with three instance models: In order to better show the label distribution, we render the labels on both vertices and polygons by using linear interpolations. So the labeled models are displayed in a continuous fashion. The black box delineates the nose feature region.

7. Conclusions and future work

We proposed a system for recognizing human faces based on the 3D model labeling technique. The generated 3D facial models derived from two facial views and the label-based feature space have shown to perform well for characterizing the individuals' 3D features. The system achieved a 92% correct recognition rate at the fourth rank and 9% equal error rate when 72 models were tested. The proposed work has certain existing implications and practices: (1) image pairs (frontal and profile views) are the most commonly used data source for personal records, which are available from existing police and federal government databases. (2) The setup of two surveillance video cameras (front and profile) to simultaneously capture two views of a face is feasible in many public sites, such as security entrances and check-in points in airports and federal government buildings, where each individual must pass through a security gate or check point one-by-one. The performance of our system relies on the quality of the reconstructed 3D models. Low quality of input images will degrade the accuracy of the individual model representation, and may increase the rate of misclassification. Our future work is to design a better feature selection algorithm, by incorporating multiple feature descriptors combined with normal maps, curvature maps, and label maps together and by using a multi-classifier strategy [20] to enhance the system performance.

Currently, our 3D face model database contains 105 face models. Our future work is to expand the existing database to a large scale and to conduct the intensive test for the data obtained under variable imaging conditions (e.g., various face sizes, variable lighting conditions and poses, etc.). We plan to compare our system with range data based systems (e.g., the reports in FRGC[25]) for performance improvement in the future.

8. Acknowledgement

We would like to thank the National Science Foundation for the support of this work under a grant IIS-0414029. We would also like to thank Dr. Jonathan Phillip for providing the FERET datasbase for our test.

References

[1] W. Zhao, R. Chellappa, A. Rosenfeld and P. J. Phillips."Face Recognition: A Literature Survey," *CVL Technical Report*, University of Maryland, Oct. 2000.

[2] G. Gordon. "Face Recognition Based on Depth and Curvature Features," *IEEE International Conference on Computer Vision and Pattern Recognition,* p808-810, 1992

[3] P. J. Phillips, H. Moon, S. A. Rizvi, and P. J. Rauss. "The FERET Evaluation Methodology for Face-Recognition Algorithms," *IEEE Trans. on Pattern Analysis and Machine Intelligence*, 22(10), 2000.

[4] X. Lu, R. Hsu, A. K. Jain, B. Kamgar-parsi, and B. Kamgarparsi. "Face Recognition with 3D Model-based Synthesis," *Intern. Conf. on Biometric Authen. (ICBA)*, pp. 139-146, 2004.

[5] H. Tanaka, M. Ikeda and H. Chiaki, "Curvature-based face surface recognition using spherical correlation," *IEEE International Conference on Face and Gesture Recognition*, pp. 372-377, 1998.

[6] J. Huang, V. Blanz, and B. Heisele. "Face Recognition with Support Vector Machines and 3D Head Models," *International Workshop on Pattern Recognition with Support Vector Machines (SVM2002),* Niagara Falls, Canada, p334-341, 2002.

[7] A Moreno, A. Sanchez, J. F. Velez, and F. J. Diaz. "Face recognition using 3D surface-extracted descriptors," *Irish Machine Vision and Image Processing Conference (IMVIP 2003).*

[8] T. Heseltine, N. Pears, and J. Austin. "Three Dimensional Face Recognition: An Eigensurface Approach," http://www-users.cs.york.ac.uk/∼tomh/

[9] V. Blanz, and T. Vetter. "Face Recognition Based on Fitting a 3D Morphable Model," *IEEE Transactions on Pattern Analysis and Machine Intelligence*, 25(9): 1063-1074, 2003.

[10] K. Chang, K. W. Bowyer, P. J. Flynn, and X. Chen. "Multibiometrics Using Facial Appearance, Shape, and Temperature," *IEEE International Conference on Face and Gesture Recognition*, May 2004.

[11] T. Heseltine, N. Pears, and J. Austin. "Three Dimensional Face Recognition: A Fishersurface Approach," *IEEE International Conference of Image Processing,* Oct. 2004.

[12] C. Zhang and F. Cohen, "3-D face structure extraction and recognition from images using 3-D morphing and distance mapping", *IEEE Transactions on Image Processing,* Nov., 2002. p1249 –1259,

[13] H. Ip, and L. Yin. "Constructing a 3DIndivisualized Head Model from Two Orthogonal Views," *The Visual Computer,* 12, Springer-Verlag, pp 254-266. 1996

[14] http://www.itl.nist.gov/iad/humanid/feret/feret_master.html, The FERET Database.

[15] R. Hsu, and A. Jain, "Face Modeling for Recognition",*International Conference on Image Processing (ICIP)* , pp. 693-696, Greece, October 7-10, 2001.

[16] A. Ansari and M. Abdel-Mottaleb, "3-D Face Modeling Using Two Views and a Generic Face Model with Application to 3-D Face Recognition", *IEEE Conf. on AVSS'03*, 2003.

[17] J. Goldfeather and V. Interrante, "A Novel Cubic-Order Algorithm for Approximating Principal Direction Vectors.", *ACM Transactions on Graphics,* Vol. 23, No. 1, January 2004, pp. 45-63.

[18] A.M. Bronstein, M.M. Bronstein and R. Kimmel, "Expression Invariant 3D Face Recognition", *Proceedings of 4th International Conference, AVBPA 2003*

[19] D. Goldberg, "Generic and Evolutionary Algorithms Come of Age", *Communications of the ACM,* 37(3): 113-119, 1994

[20] J. Czyz, J. Kittler and L. Vandendorpe, "Combining face verification experts", *Proc. International Conference on Pattern Recognition,* Vol. 2, 2002, pp. 28-31.

[21] A. Godil, S. Ressler and P. Grother, "Face Recognition using 3D surface and color map information: Comparison and Combination", *SPIE's symposium on Biometrics Technology for Human Identification,* April 12-13, 2004, Orlando, FL.

[22] http://www.ee.surrey.sc.uk/Research/VSSP/xm22vtsdb/, The XM2VTS Database.

[23] http://www.nvcc.edu/home/elanthier/methods/correlation.htm

[24] G.Van Dijck, M.M. Van Hulle, and M. Wevers, "Genetic Algorithm for Feature Subset Selection with Exploitation of Feature Correlations from Continuous Wavelet Transform: a real-case Application",*International Journal of Computational Intelligence,* 1(1) 2004,pp. 1-12.

[25] P. J. Phillips, P. J. Flynn, T. Scruggs, K. W. Bowyer, J. Chang, K. Hoffman, J. Marques, J. Min, and W. Worek, "Overview of the Face Recognition Grand Challenge," *In Proceedings of IEEE Conference on Computer Vision and Pattern Recognition,* 2005.